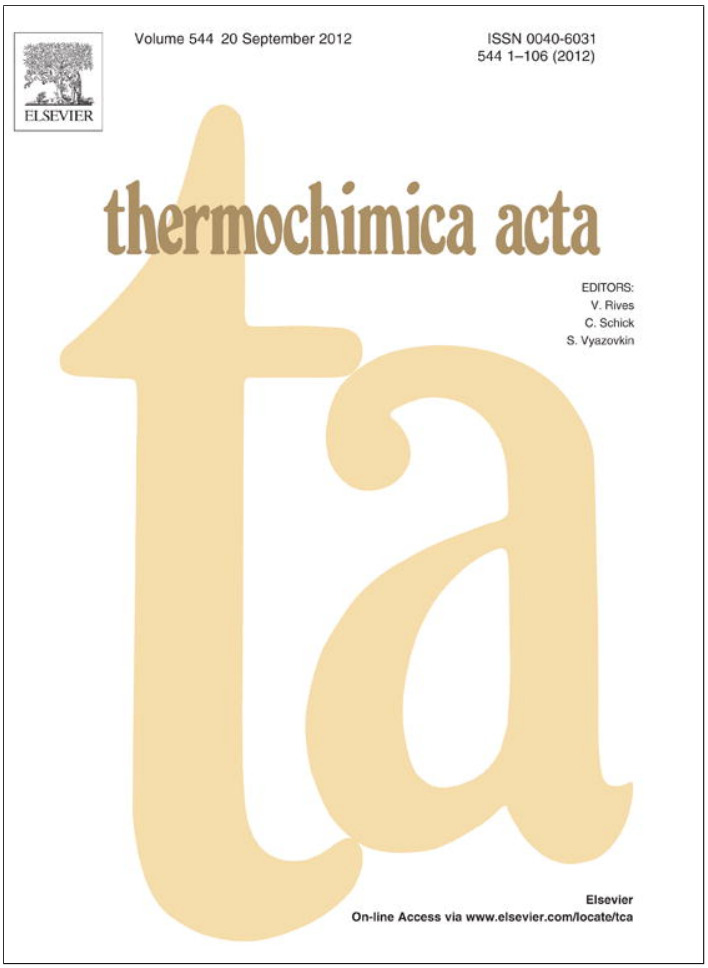

Thermochimica Acta 544 (2012) 47–53

Contents lists available at SciVerse ScienceDirect

Thermochimica Acta

journal homepage: www.elsevier.com/locate/tca

Crystallization behavior of poly(3-hydroxybutyrate) nanocomposites based on modified clays: Effect of organic modifiers

David A. D'Amico, Liliana B. Manfredi, Viviana P. Cyras *

INTEMA – Instituto de Investigaciones en Ciencia y Tecnología de Materiales, Facultad de Ingeniería, Universidad Nacional de Mar del Plata, J.B. Justo 4302, Mar del Plata, Argentina

ARTICLE INFO

Article history:
Received 19 March 2012
Received in revised form 7 June 2012
Accepted 12 June 2012
Available online 21 June 2012

Keywords:
Polyhydroxybutyrate
Clay
Biodegradable nanocomposites
Crystallization kinetic

ABSTRACT

Isothermal and non-isothermal crystallization kinetics of nanocomposites of poly(3-hydroxybutyrate) (PHB) with 4 wt% of montmorillonite Cloisite®Na^+ (CNa^+) and chemically modified clays Cloisite®15A and 93A (C15A and C93A) prepared by solution casting have been investigated by differential scanning calorimetry.

Nanoparticles addition did not significantly affect the crystallinity and melting temperatures of the PHB, regardless the type of clay.

Several models such as the Liu-Mo, Avrami, Lauritzen–Hoffman and isoconversional were found to provide a fairly satisfactory description of the crystallization kinetics of PHB and its nanocomposites.

The results showed a slight effect of the CNa^+ and C93A on the crystallization kinetics parameters of PHB. However, a retarded effect on the crystallization rate of the polymer was found when C15A clay was added. It was attributed to the high dispersion of this clay in the polymer.

Consequently, the dispersion and type of clay influence the crystallization kinetics of PHB.

1. Introduction

Poly(hydroxybutyrate) (PHB) is produced as intracellular storage materials by different types of microorganisms from renewable sources, under limited culture conditions. In the presence of an abundant source of carbon under limited nitrogen atmosphere, some bacteria can accumulate up to 60–80% of their weight in the PHB. For this reason, the PHB does not contain any residues of catalysts like other synthetic polymers. PHB is fully biodegradable polyester with optical activity and piezoelectricity. It is a hydrophobic and a highly crystalline polymer with an elevated melting temperature. It is still expensive, quite stiff, brittle and has a narrow processability window. The degree of its brittleness depends on the degree of crystallinity, glass transition temperature and microstructure [1–3].

Preparation of nanocomposites, using low percentages of inorganic fillers, is among the routes to improve some of the properties of biodegradable polymers such as thermal, mechanical and oxidative barrier, when they are compared with traditional composites. Montmorillonite is among the most commonly used layered silicates inorganic filler because it is environment friendly and readily available in large quantities with relatively low cost [4–7].

The polymer properties depend on the crystallization conditions, and thus the crystallization kinetics. The introduction of clay plays a significant role in the properties of polymers, due to the influence of the nanoparticles on their morphology and crystallization behavior [2]. So, it is very useful to characterize the nucleation, crystallization and structural development of PHB in clay reinforced polymer nanocomposites. This characterization should be used to optimize the processing conditions for achieving high performance polymer nanocomposites as well as realize full potential applications of these materials.

For the purpose of describing the evolution of crystallinity under isothermal or dynamical conditions, a number of mathematical models have been proposed [8], based on the notion of primary nucleation and subsequent crystal growth mechanisms. In this case, we used the Liu-Mo theory to model the dynamical scans, and the Avrami equation, Lauritzen–Hoffman model and isoconversional method to analyze the isothermal results.

In this work, an extensive study of the crystallization kinetics of clay/polymer nanocomposites was done in order to understand the influence of different clays on the crystallization behavior of PHB. The isothermal and non-isothermal behavior will be important for predicting the crystallization behavior of the materials according to the organic modifier of the nanoparticle.

* Corresponding author.
E-mail addresses: lbmanfre@fi.mdp.edu.ar (L.B. Manfredi), vpcyras@fi.mdp.edu.ar (V.P. Cyras).

0040-6031/$ – see front matter © 2012 Elsevier B.V. All rights reserved.
http://dx.doi.org/10.1016/j.tca.2012.06.012

Table 1
Organic modifier and the interlayer distance of the clays.

Clay	Cloisite®Na^+ (CNa^+)	Cloisite®93A (C93A)	Cloisite®15A (C15A)
Organic modifier	–	CH_3 | $H-N^+-HT$ | HT	CH_3 | CH_3-N^+-HT | HT
d(0 0 1)	11.7 Å	23.6 Å	31.5 Å

2. Materials and experimental methods

2.1. Materials

A biodegradable polymer, polyhydroxybutyrate (PHB) (Mn = 42,500) was kindly supplied by PHB Industrial S.A., Brazil. Montmorillonite Cloisite®Na^+, organically modified Cloisite®C15A and Cloisite®C93A were supplied by Southern Clay Products (TX, USA). The organic modifier and the interlayer distance of the clays are shown in Table 1.

Films of PHB and its nanocomposites were obtained by casting process. A homogeneous solution of PHB in chloroform was prepared by stirring at 450 rpm while heating at 60 °C, for 15 min. Then, the solution was placed on glass Petri dishes and it was allowed to evaporate at room temperature. Nanocomposites were prepared by the addition of a chloroform clay solution, previously sonicated, to the PHB solution. The solution was evaporated following the procedure previously mentioned. Nanocomposites contained 4% (w/w) of each kind of montmorillonite. All films were stored in a desiccator at room temperature for 30 days to allow complete crystallization of PHB [9]. The film thickness of PHB and nanocomposites was 0.05 mm.

2.2. Methods

2.2.1. X-ray diffraction analyses (XRD)

XRD analyses were performed with CuKα (λ = 1.54 Å) radiation in a Philips PW 1710 X-ray diffractometer system. Every scan was recorded in the range of $2\theta = 2–60°$ at a scan speed of 2°/min with an X-ray tube operated at 40 kV and 40 mA [4].

2.2.2. Differential scanning calorimetry (DSC)

Thermal behavior and crystallization kinetics were performed using a Perkin-Elmer Pyris 1 DSC. About 5–8 mg of sample was sealed in an aluminum pan, and all scans were carried out under inert nitrogen (20 ml min^{-1}).

The melting temperature and the overall crystallinity of the samples were obtained leading one scan from room temperature to 200 °C at a rate of 10 °C/min.

The overall crystallinity was calculated according to the following equation:

$$X_c\ (\%) = \frac{\Delta H_m (m_c/m_p)}{\Delta H_0} \times 100 \quad (1)$$

where ΔH_m is the melting enthalpy measured from heating experiments, ΔH_0 is the theoretical enthalpy of 100% crystalline PHB (ΔH_0 = 146 J/g [10]), m_c is the nanocomposite weight and m_p is the weight of PHB in the nanocomposite.

The non-isothermal crystallization behavior of PHB and its nanocomposites was studied by cooling the samples from 195 °C to room temperature at constant rates of 2.5, 5, 10, 12.5 and 15 °C/min. It should be noted that it was necessary to melt the sample at 195 °C for at least 1 min to erase its previous thermal history as well as to avoid its thermal degradation, as it was found in our previous work [9].

The isothermal crystallization experiments were done by heating the sample from −30 °C to 195 °C at a scanning rate of 30 °C/min and holding it temperature for 1 min. Then, the sample was quenched to a desired isothermal crystallization temperature T_C, at a cooling rate of 80 °C/min. It was assumed that the crystallization was finished when the exothermic trace converged to a horizontal baseline. After that, the melting temperature of the samples crystallized at T_C, was obtained leading a scan from room temperature to 200 °C at a rate of 10 °C/min.

3. Results and discussion

3.1. X-ray diffraction analyses (XRD)

In general, the crystallization behavior of nanocomposites is strongly influenced by the dispersion state of nanolayers in polymer matrix [11,12], which can be analyzed from X-ray diffraction analyses. Fig. 1 shows the X-ray spectra of the PHB and its nanocomposites films. At lower angles, the peaks corresponding to the clay interlayer region could be observed in the nanocomposites profiles. The d(0 0 1) diffraction peak of all the pristine clays was shifted to lower angles when they were added to the PHB, showing that the clay intergallery region was expanded. Comparing the composites containing the modified clays, C93A showed a higher peak than C15A in the 2θ region between 2° and 5°. This suggests that most of the C93A clay has an interlayer distance of 28.5 Å, corresponding to the peak at 3.1°. Though as there is only a small peak in the 2–5° spectra region of C15A, most of this clay should have an interlayer distance higher than 44 Å ($2\theta = 2°$) that cannot be observed in the spectra. So, it seems that C15A was better dispersed in the PHB than C93A. The rest of the spectra pattern is very similar among the materials studied, which is indicative of the similar crystalline morphology of PHB in spite of the clay added.

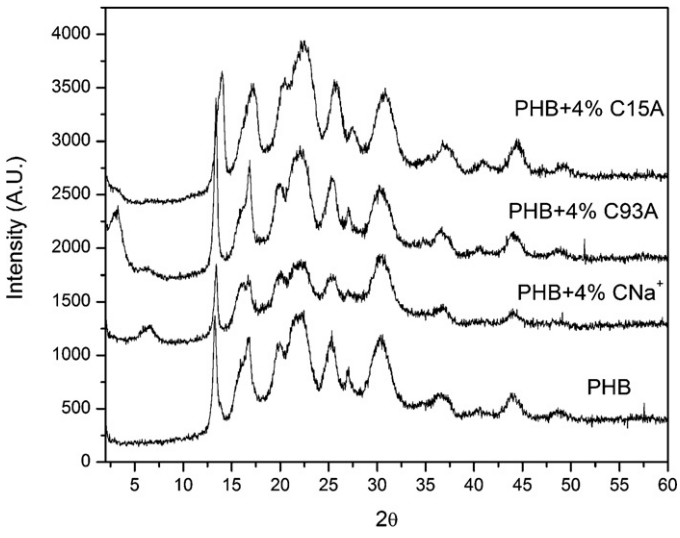

Fig. 1. XRD of PHB and its nanocomposites.

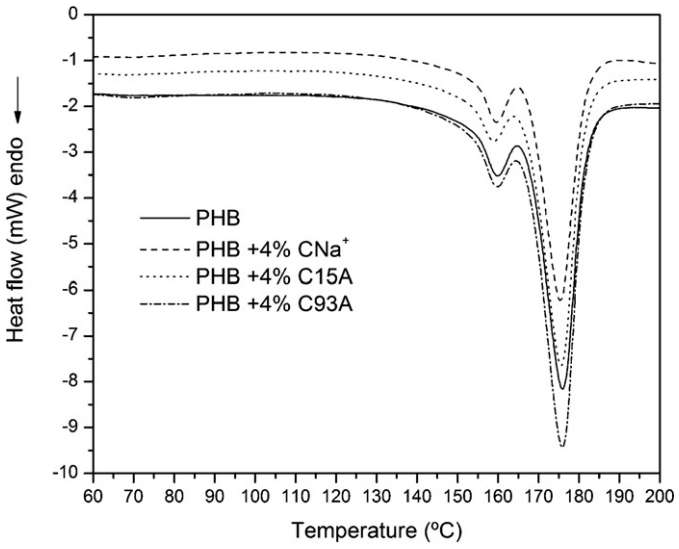

Fig. 2. DSC melting curves of PHB and its nanocomposites.

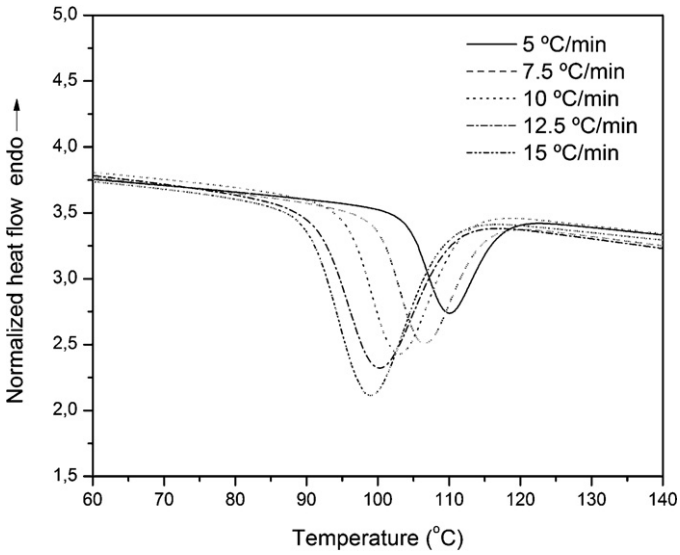

Fig. 3. DSC dynamic scans of PHB at different heating rates.

3.2. Thermal behavior of PHB films and its nanocomposites

In order to study the thermal behavior of PHB films and its nanocomposites, dynamic DSC thermograms were performed (Fig. 2). The fusion temperature (T_m) and the percentage of crystallinity (X_c) were calculated from those curves and summarized in Table 2. It was observed that the clay incorporation had a little effect on the crystallinity and melting temperature of PHB. This was probably because the clay is predominantly confined to the amorphous phase, without significantly affecting the development of crystals in the polymer matrix. In this way, the glass transition temperature of the PHB increased with the addition of the different clays, resulting from the hindrance of segmental motion of the PHB chains by the clay.

3.3. Non-isothermal crystallization behavior

Fig. 3 shows the curves of the heat flow as a function of temperature during the non-isothermal crystallization of PHB in a DSC, at the selecting five speeds of cooling rate. The crystallization peak temperature (T_C) of PHB decreases with the increase of the cooling rate and the same result was obtained for its different nanocomposites. Additionally, comparing the nanocomposites behavior, it was observed that the T_C of the nanocomposites was higher than that of the PHB, except for the composite containing C15A, indicating a slow rate of crystallization in the latter case.

From the DSC assays, the relative degree of crystallinity, $\alpha(T)$, as a function of temperature can be calculated as follows (Eq. (2)):

$$\alpha(T) = \frac{\int_{T_0}^{T} dH_c/dT}{\int_{T_0}^{T\infty} dH_c/dT} \quad (2)$$

where T_0 and T_∞ are the initial and final crystallization temperatures, respectively.

Table 2
Thermal properties of the materials studied.

Material	T_m (°C)	T_g (°C)	X_c
PHB	175.9	−5.8	66.5%
PHB + 4% CNa^+	175.7	−3.7	66.2%
PHB + 4% C93A	176.1	−2.5	65.1%
PHB + 4% C15A	175.7	−2.3	65.9%

The $\alpha(T)$ curves versus temperature for the PHB and its different nanocomposites at a rate of 5 °C/min are shown in Fig. 4. Those curves of experimental data showed a sigmoidal shape, similar among the materials, as well as the slow rate of crystallization of the nanocomposite containing C15A clay.

To study the non-isothermal crystallization kinetics, several theoretical models were used [8,13–15]. One of them is the theory proposed by Liu-Mo [16]. This method is used to connect the Avrami equation with the Ozawa equation.

In the Avrami model, the relative degree of crystallinity, $\alpha(T)$, is related to the crystallization time, t, as:

$$\alpha(t) = 1 - \exp(Z_t t^n) \quad (3)$$

where n is the Avrami exponent and Z_t (where $Z_t = z_t^n$) is the crystallization rate constant involving both nucleation and growth rate parameters. This theory provides useful data on the overall crystallization kinetics. The parameters, n and Z_t, can be used to interpret qualitatively the nucleation mechanism, morphology and the overall crystallization rate of the polymer.

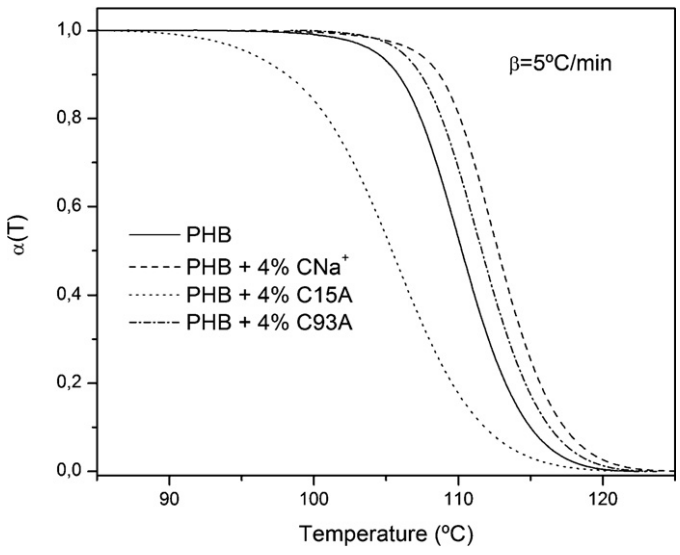

Fig. 4. Relative degree of crystallinity vs. temperature for PHB and its nanocomposites.

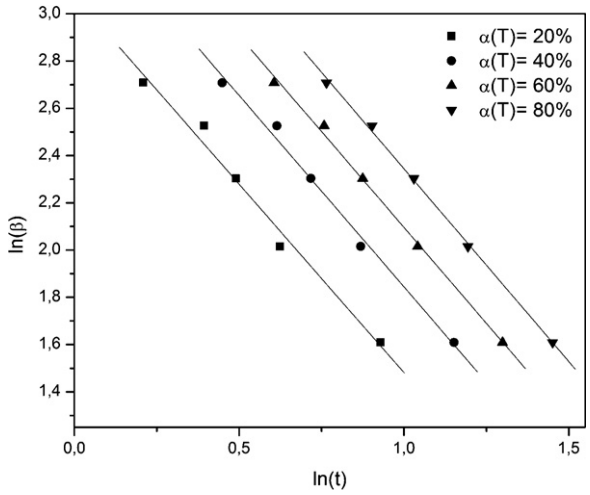

Fig. 5. Plots of ln(β) as a function of ln(t), PHB + 4% C15A.

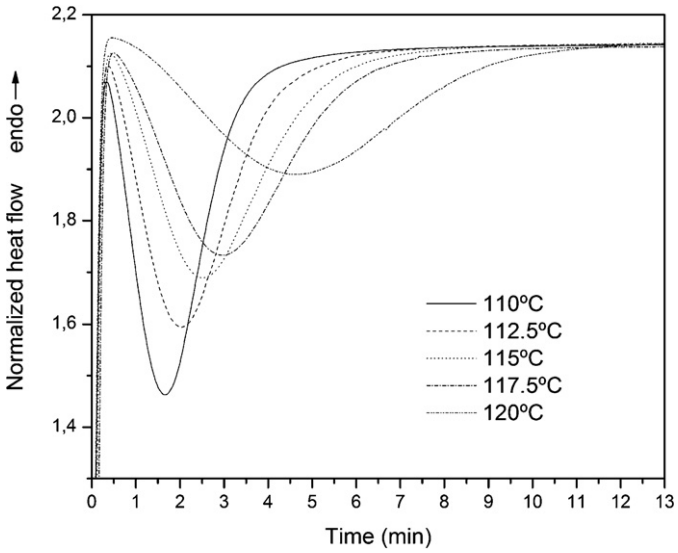

Fig. 6. DSC thermograms of isothermal crystallization at different crystallization temperatures to PHB + 4% C15A.

The theory proposed by Ozawa describes the effect of the cooling rate on the crystallization from the melt by replacing the time variable in the Avrami equation with a variable cooling rate term as follows:

$$\alpha(T) = 1 - \exp\left(\frac{-K(T)}{\beta^m}\right) \quad (4)$$

$$\ln[-\ln\{1-\alpha(T)\}] = \ln\ K(T) - m\ln(\beta) \quad (5)$$

where $\alpha(T)$ is the relative degree of crystallinity, $K(T)$ is a cooling function related to the crystallization rate, m is the Ozawa exponent depending on the dimension of crystal growth and β is the cooling rate.

So, the Avrami equation relates α with t and the Ozawa equation relates it with β, thus the relation between β and t can be used to connect both equations. Then, the expressions obtained from the combination of both models are shown in Eqs. (6)–(8):

$$\ln(Z_t) + n\ \ln(t) = \ln[K(T)] - m\ \ln(\beta) \quad (6)$$

$$\ln(\beta) = \frac{1}{m}\ \ln\left[\frac{K(T)}{Z_t}\right] - \frac{n}{m}\ \ln(t) \quad (7)$$

$$\ln(\beta) = \ln[F(T)] - a\ \ln(t) \quad (8)$$

where the kinetic parameter $F(T) = [K(T)/Z_t]^{1/m}$, represents the value of cooling rate chosen at a unit crystallization time when the systems have a defined degree of crystallinity; β is the cooling rate, and a is the ratio of the Avrami exponent (n) to the Ozawa exponent (m) [16].

Plotting ln(β) versus ln(t), to a certain degree of crystallinity (20%, 40%, 60% and 80%) it is possible to determine the values of $F(T)$, from the intercept of the lines (Fig. 5). It can be seen that these plots show good linearity. The physical meaning of $F(T)$ is the cooling rate that must be selected to achieve the system a given degree of crystallinity within a unit of crystallization time.

The values of $F(T)$ calculated for the PHB and its nanocomposites are listed in Table 3. The bigger the value of $F(T)$, the higher the degree of crystallinity. In general, the $F(T)$ values of the nanocomposites were similar to the one of the PHB, except for the composite containing C15A, that were higher. These findings indicated that the addition of the clay C15A lowered the crystallization rate. It is consistent with the results showed in Fig. 4, where the curves of the PHB and the composites containing CNa^+ and C93A were similar among them; whereas the PHB/C15A curve was markedly displaced to the left.

Table 3
$F(T)$ values for the different materials studied.

% $\alpha(T)$	PHB	PHB + 4% CNa^+	PHB + 4% C15A	PHB + 4% C93A
20	2.49	2.56	3.19	2.52
40	2.85	2.81	3.60	2.90
60	3.07	3.00	3.92	3.16
80	3.27	3.17	4.18	3.39

3.3.1. Nucleation activity (φ)

Dobreva et al. [17] has developed an equation for calculating the nucleation activity (φ) of different substrates during the non-isothermal crystallization of polymer melts. If the reinforcement is extremely active, the nucleation activity will tend to zero, while for inert reinforcement, it will be close to one.

For nucleation from the melt, the cooling rate is represented by Eq. (9) at temperatures close to melting:

$$\ln\ \beta = A - \left[\frac{B}{\Delta T_c{}^2}\right] \quad (9)$$

where β is the cooling rate, A is a constant, ΔT_C ($=T_m - T_c$) is the degree of subcooling, T_c is the temperature corresponding to the peak temperature of DSC crystallization, T_m is the melting temperature and B is a parameter related to the three dimensional nucleation. The value of B for the pure polymer and its nanocomposites (B^*) was obtained from Eq. (9). Then, φ can be calculated by Eq. (7):

$$\varphi = \left[\frac{B^*}{B}\right] \quad (10)$$

The calculated values of the nucleation activity were between 0.76 (for the composites containing CNa^+ and C93A) and 1.01 (for the composites containing C15A). It showed a slight nucleating activity of CNa^+ and C93A clays, while an inert behavior of the C15A.

3.4. Isothermal crystallization behavior

The DSC crystallization exotherms for the PHB and its nanocomposites that had been isothermally crystallized at different crystallization temperatures (T_C) are shown in Fig. 6.

In order to analyze the isothermal crystallization process, the crystallization kinetics of PHB and its nanocomposites was compared. The curves of α as a function of crystallization time t for the PHB and its nanocomposites, at $T_C = 112\ ^\circ C$, are reported in Fig. 7, as

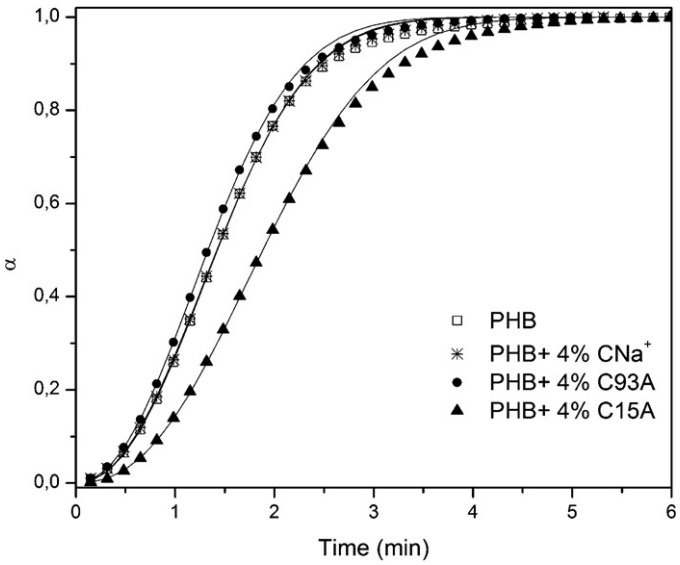

Fig. 7. The relative degree of crystallinity with time for the crystallization of PHB.

an example. By using Eq. (2) modified to isothermal experiments, α was calculated from the curves of heat flow versus time at different T_C (Fig. 6).

The crystallization rate of the nanocomposites increased with the decrease of T_C, due to the higher supercool degree. The plots of α versus time for the PHB and nanocomposites are similar among them, showing a sigmoidal shape. It was observed that the presence of C15A clay retarded the crystallization phenomenon.

The crystallization half-time ($t_{1/2}$) obtained from the isothermal crystallization curves of pure PHB and the PHB/clay nanocomposites is shown in Fig. 8. This time corresponds to the necessary polymer to reach 50% of its maximum crystallinity. In general, the value of $t_{1/2}$ for pure PHB and the PHB/clay nanocomposites increases with increasing the temperature of crystallization. It was observed that the $t_{1/2}$ values of the PHB nanocomposites with C93A and CNa^+ were slightly lower than that of pure PHB. This result indicated that the incorporation of C93A and CNa^+ slightly increased the crystallization rate of the PHB matrix. In other hand, the value of $t_{1/2}$ of PHB/C15A was higher than that of pure PHB, indicating retardation in the crystallization rate of the polymer due to the C15A addition.

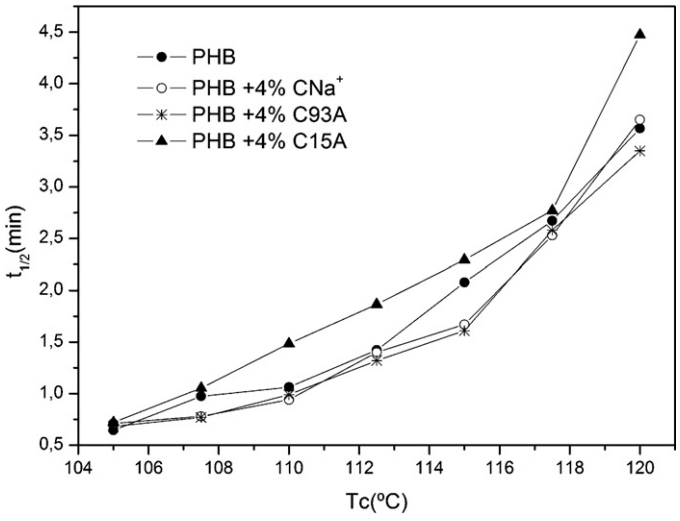

Fig. 8. Crystallization half-time vs T_C for PHB and its nanocomposites.

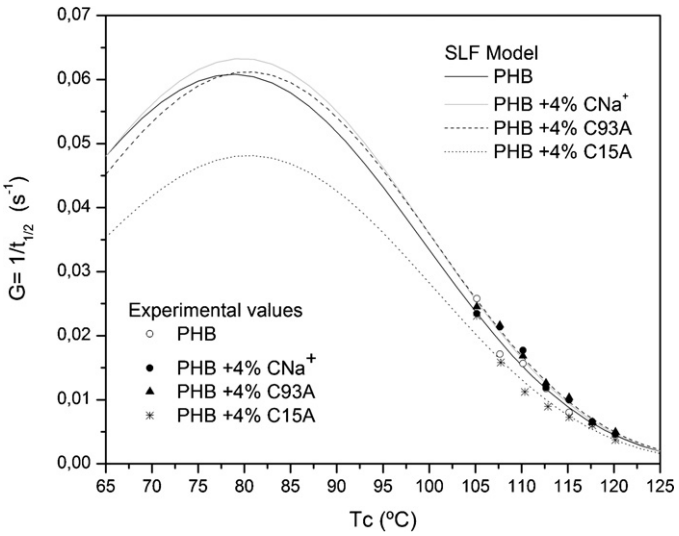

Fig. 9. Overall rate of crystallization as a function of T_C calculated from experimental data and SLF model.

The reciprocal value of $t_{1/2}$ is assumed to be equal to the experimental rate ($G \approx 1/t_{1/2}$) of the isothermal crystallization [18]. It can be noted in Fig. 9 that the crystallization rate decreased with the increment of T_C, since it is closer to T_m, and it was low when the C15A clay was added to the PHB.

The Lauritzen–Hoffman model [18] was widely used to determine the dependence of the overall rate of crystallization, G, on the crystallization temperature. The model expression is the following:

$$G = G_0 \exp\left(\frac{-U}{R(T - T_\infty)}\right) \exp\left(\frac{-K_G}{fT\,\Delta T}\right) \quad (11)$$

where G_0 is a constant independent of temperature; U is the activation energy for the transport of crystallizable segments; T_∞ is a hypothetical temperature at which molecular motion associated with viscous flow is stopped and is related to T_g, as $T_\infty = T_g - C$, where C is a constant; ΔT is the degree of subcooling, given by $T_{m0} - T_c$, where T_m is the melting temperature in equilibrium; R is the gas constant; f is a factor representing the variation of enthalpy in the molten unit volume with temperature, given by $f = 2T/(T_m + T)$; and K_G is the constant of nucleation [19]. In the present work, K_G was calculated using the nucleation Lauritzen–Hoffman equation constants modified by Suzuki (SLF method), where $C = 30$ K and $U = 1500$ cal/mol. The values of T_{m0} were reported in Table 4. The plot of the expression of SLF is shown in Fig. 9, where it was observed a good correlation with the experimental data. The fit allows to predict the behavior of the system in the whole range of temperature, which is helpful because it is not easy to be experimentally measured for PHB at low temperatures [20].

In order to fully understand the evolution of crystallinity during the isothermal crystallization, the Avrami model (Eq. (3)) was also employed to analyze the crystallization kinetics of PHB and its nanocomposites [20]. By fitting the experimental data, n and Z_t values can be obtained from the plots of the linearized form of the Avrami equation:

$$\ln\{-\ln[1 - \alpha]\} = \ln Z_t + n \ln t \quad (12)$$

Table 4 displays the values of Z_t and n of the PHB and its nanocomposites, calculated by the Avrami model. The constants n of the materials studied, which represents the nucleation mechanism and crystals growth dimension, varies from 2.64 to 1.87, indicating a two-dimensional growth of crystals. The presence of nanoclay did not show a notable influence on the crystallization mechanism of the pure PHB, having the nanocomposites with C15A the lowest

Table 4
Values of T_c, T_{m0}, Z_t, n and E_a from the Avrami method.

Materials	T_c (°C)	n_{Avrami}	Z_t	E_a	T_{m0} (°C)
PHB	105	1.87	1.5593	−133.56 (r^2 = 0.99)	185.8
	107.5	2.08	0.7509		
	110	2.03	0.5866		
	112.5	2.23	0.3149		
	115	2.45	0.1165		
	117.5	2.57	0.0547		
	120	2.52	0.0281		
PHB + 4% CNa^+	105	1.91	1.2863	−131.85 (r^2 = 0.98)	182.4
	107.5	1.89	1.0857		
	110	2.1	0.7519		
	112.5	2.19	0.3218		
	115	2.32	0.2091		
	117.5	2.54	0.0652		
	120	2.64	0.0223		
PHB + 4% C93A	105	1.89	1.4704	−130.76 (r^2 = 0.99)	183.8
	107.5	1.97	1.1106		
	110	2.08	0.6944		
	112.5	2.17	0.3737		
	115	2.34	0.227		
	117.5	2.5	0.0651		
	120	2.61	0.0293		
PHB + 4% C15A	105	2.29	1.3185	−135.13 (r^2 = 0.98)	181.5
	107.6	2.31	0.5864		
	110.2	2.39	0.2784		
	112.7	2.37	0.1544		
	115	2.40	0.0899		
	117.5	2.42	0.0607		
	120	2.52	0.0159		

values of Z_t. The experimental data were fit using these parameters and it was observed a good correlation with the Avrami predictions (straight lines in Fig. 7). The n and Z_t values were between the ones obtained by other authors, i.e. n value between 1.5 and 3.0 [15,20,21].

The simplification of the classical temperature dependence of Z_t, previously proposed [22] can be used in order to calculate the effective activation energy:

$$Z_{ti} = Z_{t0} \exp\left[\frac{-E_a}{RT_C}\right] \quad (13)$$

where Z_{t0} is the temperature independent preexponential factor, R is the gas constant, T_C is the crystallization temperature and E_a is the crystallization activation energy.

The value of the activation energy of the PHB nanocomposites with C93A and CNa^+ was slightly higher than that of pure PHB. However, the value corresponding to PHB/C15A was somewhat lower than that of pure PHB. As these activation energy values represent the energy of the overall crystallization process, this could be the reason of the mismatch with the previous results (nucleation and $t_{1/2}$).

Then to elucidate this finding, the effective activation energy was calculated through the model-free isoconversional method, which accounts for its dependence on the whole range of the relative degree of crystallinity [8]. Isoconversional analysis was performed by modifying Eq. (13) for an isothermal process, obtaining Eq. (14):

$$\left[\frac{\partial \ln(d\alpha/dt)}{\partial T^{-1}}\right]_\alpha = \left[\frac{\partial \ln(k(T))}{\partial T^{-1}}\right]_\alpha + \left[\frac{\partial \ln f(\alpha)}{\partial T^{-1}}\right]_\alpha \quad (13')$$

$$\ln t_{\alpha,i} = \ln\left[\frac{g(\alpha)}{A}\right] + \frac{E_\alpha}{RT_i} \quad (14)$$

where $g(\alpha)$ is the integral form of the kinetic model, t is the time, T is the temperature, A is a constant, R is the gas constant and E_α is the isoconversional effective activation energy. From the slope of the plot of $\ln t_{\alpha,i}$ vs $1/T_i$, E_α values of the samples were obtained at each α, without assumption of a kinetic model. Fig. 10 describes the variation of the activation energy of PHB and its nanocomposites with the relative degree of crystallinity. The average values of the apparent activation energy (E_a) using Avrami methods were very close to the values of the effective activation energy (E_α) calculated by isoconversional method. The activation energy of PHB, PHB + 4% CNa^+ and PHB + 4% C93A increase with the relative crystallinity, in a similar way. This suggests that the crystallization of PHB and these nanocomposites becomes more difficult as crystallization progresses. Instead, the activation energy of nanocomposite with C15A remained almost unchanged with the degree of crystallinity. However, its value of the effective activation energy is the highest at the beginning of the crystallization process. This could be

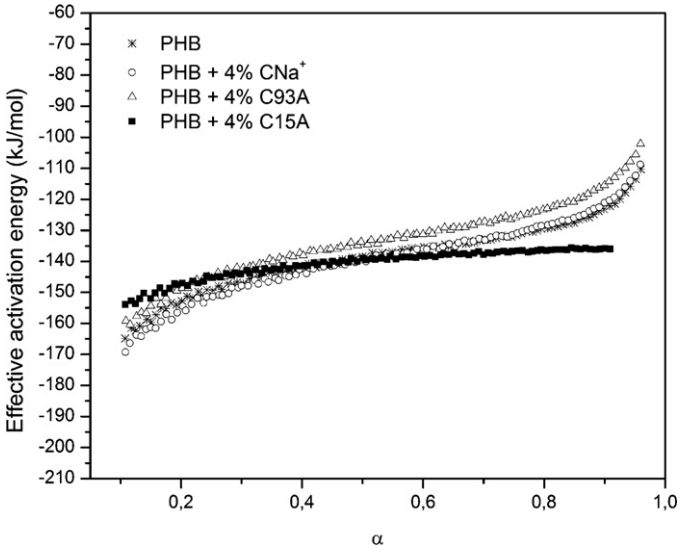

Fig. 10. Activation energy of PHB and its nanocomposites varying with relative crystallinity.

associated with a decrease in the diffusion rate of polymer molecules [23] in the most tortuous morphology due to the good dispersion of C15A in the PHB, as it was observed in the DRX patterns. These results are now in accordance with the above results related to the nucleation activity and $t_{1/2}$.

4. Conclusions

In order to analyze the influence of the clays on the kinetic of crystallization and crystallinity of the PHB, nanocomposites based on PHB and 4% (w/w) of different types of clays were obtained.

It was found that the nanoparticles addition had a little effect on the crystallinity degree and melting temperature of the PHB, regardless of the type of clay used. However, the nanocomposites glass transition temperature was higher than the one of PHB, probably due to the steric hindrance caused by the clays. In addition, the PHB crystalline structure was not modified by the clays, as it was observed by DRX.

To study the crystallization kinetics, several isothermal and non-isothermal theoretical models were used.

From non-isothermal analysis it was observed a retarded effect on the crystallization kinetics of the PHB when C15A clay was added to the polymer, due to the diminution in the crystallization peak temperature and the increment of the Liu-Mo parameter. On the other hand, a slight effect of the CNa^+ and C93A on the kinetic parameters was found. Additionally, the use of isothermal kinetics models gave similar results about the influence of the type of clay on the crystallization rate of PHB.

Therefore, it can be concluded that the incorporation of the C15A clay decreases the crystallization rate of PHB chains, without changing the level of crystallinity. The crystallization effective activation energy of nanocomposite with C15A remained nearly unchanged with the degree of crystallinity, but having the highest value at the beginning of crystallization process. It was related to the best dispersion of this type of clay in the polymer, as it was observed in the DRX patterns. So, the crystallization kinetics was greatly affected by the dispersion and the organic modifiers of the clays.

Acknowledgments

The authors gratefully acknowledge the support from the National Research Council of Argentina (CONICET) - PIP 014 and the National University of Mar del Plata.

References

[1] V.P. Cyras, A. Vázquez, Ch. Rozsa, N. Galego Fernandez, L. Torre, J.M. Kenny, Thermal stability of P(HB-co-HV) and its blends with polyalcohols: crystallinity, mechanical properties and kinetic of degradation, J. Appl. Polym. Sci. 77 (2000) 2889–2900.
[2] P. Bordes, E. Pollet, S. Bourbigot, L. Avérous, Structure and properties of PHA/clay nano-biocomposites prepared by melt intercalation, Macromol. Chem. Phys. 209 (2008) 1473–1484.
[3] X. Gao, J. Chen, Q. Wu, G.Q. Chen, Polyhydroxyalkanoates as a source of chemicals, polymers, and biofuels, Curr. Opin. Biotechol. 22 (2011) 768–774.
[4] V.P. Cyras, L.B. Manfredi, M.T. Ton-That, A. Vázquez, Physical and mechanical properties of thermoplastic starch/montmorillonite nanocomposites films, Carbohydr. Polym. 73 (2008) 55–63.
[5] P. Maiti, C.A. Batt, E.P. Giannelis, Renewable plastics: synthesis and properties of PHB nanocomposites, Polym. Mater. Sci. Eng. 88 (2003) 58–59.
[6] S.T. Lim, Y.H. Hyun, C.H. Lee, H.J. Choi, Preparation and characterization of microbial biodegradable poly(3-hydroxybutyrate)/organoclay nanocomposite, J. Mater. Sci. Lett. 22 (2003) 299–302.
[7] P. Bordes, E. Pollet, L. Avérous, Nano-biocomposites: biodegradable polyester/nanoclay systems, Prog. Polym. Sci. 34 (2009) 125–155.
[8] S. Vyazovkin, A.K. Burnham, J.M. Criado, L.A. Pérez-Maqueda, C. Popescu, N. Sbirrazzuoli, Review. ICTAC Kinetics Committee recommendations for performing kinetic computations on thermal analysis data, Thermochim. Acta 520 (2011) 1–19.
[9] D.A. D'Amico, L.B. Manfredi, V.P. Cyras, Relationship between thermal properties, morphology and crystallinity of nanocomposites based on polyhydroxybutyrate, J. Appl. Polym. Sci. 123 (2012) 200–208.
[10] H.J. Chiu, Segregation morphology of poly(3-hydroxybutyrate)/poly(vinyl acetate) and poly(3-hydroxybutyrate-co-10% 3-hydroxyvalerate)/poly(vinyl acetate) blends as studied via small angle X-ray scattering, Polymer 46 (2005) 3906–3913.
[11] L. Peng, Polymer modified clay minerals: a review, Appl. Clay Sci. 38 (2007) 64–76.
[12] S. Labidi, N. Azema, D. Perrin, J. Lopez-Cuesta, Organo-modified montmorillonite/polycaprolactone nanocomposites prepared by melt intercalation in a twin-screw extruder, Polym. Degrad. Stab. 95 (2010) 382–388.
[13] S. Vyazovkin, N. Sbirrazzuoli, Isoconversional approach to evaluating the Hoffman–Lauritzen parameters (U* and Kg) from the overall rates of non-isothermal crystallization, Macromol. Rapid Commun. 25 (2004) 733–738.
[14] W. Hao, W. Li, W. Yang, L. Shen, Effect of silicon nitride nanoparticles on the crystallization behavior of polypropylene, Polym. Test. 30 (2011) 527–533.
[15] M. Erceg, T. Kovacic, I. Klaric, Poly(3-hydroxybutyrate) nanocomposites: isothermal degradation and kinetic analysis, Thermochim. Acta 485 (2009) 26–32.
[16] T.X. Liu, Z.S. Mo, S. Wang, H.F. Zhang, Nonisothermal melt and cold crystallization kinetics of poly(aryl ether ether ketone ketone), Polym. Eng. Sci. 37 (1997) 568–575.
[17] A. Dobreva, I. Gutzow, Activity of substrates in the catalyzed nucleation of glass-forming melts. II. Experimental evidence, J. Non-Cryst. Solids 162 (1993) 13–25.
[18] J.D. Hoffman, G.T. Davies, J.I. Lauritzen, Treatise on Solid State Chemistry: Crystalline and Non-Crystalline Solids, Plenum, New York, 1976.
[19] Y. Jiang-Wen, C. Hsiu-Jung, D. Trong-Ming, Spherulitic morphology and crystallization kinetics of melt-miscible blends of poly(3-hydroxybutyrate) with low molecular weight poly(ethylene oxide), Polymer 44 (2003) 4355–4362.
[20] V.P. Cyras, Ch. Rozsa, N. Galego, A. Vázquez, Kinetic expression for the isothermal crystallization of P(HB-HV), J. Appl. Polym. Sci. 94 (2004) 1657–1661.
[21] M.L. Di Lorenzo, C. Silvestre, Non-isothermal crystallization of polymers, Prog. Polym. Sci. 24 (1999) 917–950.
[22] A. Maffezzoli, J.M. Kenny, L. Nicolais, A macrokinetic approach to crystallization modelling of semicrystalline thermoplastic matrices for advanced composites, J. Mater. Sci. 28 (1993) 4994–5001.
[23] G.Z. Papageorgiou, D.N. Bikiaris, D.S. Achilias, Effect of molecular weight on the cold-crystallization of biodegradable poly(ethylene succinate), Thermochim. Acta 457 (2007) 41–54.